Carbohydrate Polymers 77 (2009) 891–897

Contents lists available at ScienceDirect

Carbohydrate Polymers

journal homepage: www.elsevier.com/locate/carbpol

Preparation, characterization and properties of superabsorbent nanocomposites based on natural guar gum and modified rectorite

Wenbo Wang [a,b], Aiqin Wang [a,*]

[a] Center for Eco-material and Green Chemistry, Lanzhou Institute of Chemical Physics, Chinese Academy of Sciences, Lanzhou 730000, PR China
[b] Graduate School of the Chinese Academy of Sciences, Beijing 100049, PR China

ARTICLE INFO

Article history:
Received 8 February 2009
Received in revised form 2 March 2009
Accepted 5 March 2009
Available online 19 March 2009

Keywords:
Superabsorbent nanocomposites
Guar gum
Rectorite
Exfoliation
Intercalation
Swelling

ABSTRACT

Novel guar gum-*g*-poly(sodium acrylate)/rectorite (GG-*g*-PNaA/REC) superabsorbent nanocomposites were prepared in aqueous solution using guar gum (GG), partially neutralized acrylic acid (NaA), acidified rectorite (H^+-REC) and organified rectorite (CTA^+-REC) by cetyltrimethylammonium bromide (CTAB) as raw materials, ammonium persulfate (APS) as initiator and *N,N′*-methylenebisacrylamide (MBA) as cross-linker. FTIR spectra confirmed that NaA had been grafted onto GG chains and the —OH groups of REC participated in polymerization reaction. Exfoliated nanocomposite was obtained for H^+-REC and intercalated structure was formed for CTA^+-REC as shown by XRD results. SEM observations show REC has been uniformly dispersed in polymeric matrix. Effects of HCl concentration, organification degree of CTA^+-REC and content of REC on swelling capabilities were investigated and the swelling kinetics of nanocomposites was evaluated. Results indicate that modifying REC by acidification and organification can improve swelling properties of the resultant nanocomposites, and GG-*g*-PNaA/CTA^+-REC exhibited higher swelling capability and swelling rate contrast to GG-*g*-PNaA/H^+-REC.

1. Introduction

Superabsorbent can absorb and retain large amounts of aqueous fluids even under some pressure compared to general absorbents, so it has exhibited potential application in many fields such as agriculture (Chu, Zhu, Li, Huang, & Li, 2006; Puoci et al., 2008), hygienic products (Kamat & Malkani, 2003; Kosemund et al., 2009), wastewater treatment (Kaşgöz, Durmus, & Kaşgöz, 2008; Wang, Zhang, & Wang, 2008) and drug-delivery (Sadeghi & Hosseinzadeh, 2008). Thus far, many kinds of materials have been used for preparing superabsorbents, among them the naturally available resources such as polysaccharides and inorganic clay minerals have shown particular advantages and drawn considerable attention (Ray & Bousmina, 2005). The utilization of low cost, annually renewable and biodegradable polysaccharides for deriving superabsorbents has offered commercial and environmental superiorities (Pourjavadi, Barzegar, & Mahdavinia, 2006; Yoshimura, Uchikoshi, Yoshiura, & Fujioka, 2005), and the incorporation of inorganic clays or their modified products has also improved the performance of the resultant materials and further reduced the production cost (Zhang, Wang, & Wang, 2007). Presently, the natural polysaccharides including starch (Lanthong, Nuisin, & Kiatkamjornwong, 2006; Li, Zhang, & Wang, 2007), cellulose (Suo, Qian, Yao, & Zhang, 2007), chitosan (Chen, Liu, Tan, & Jiang, 2009; Liu, Wang, & Wang, 2007b), alginate (Hua & Wang, 2009; Pourjavadi, Ghasemzadeh, & Soleyman, 2007a) and gelatin (Pourjavadi, Hosseinzadeh, & Sadeghi, 2007b) have been used for deriving superabsorbents, and the resultant materials have also shown potentials as substitutes for existing petroleum-based superabsorbent materials.

Guar gum (GG) is derived from the seeds of guar plant *Cyanapsis tetragonolobus* (Leguminosae); it is a natural nonionic branched polymer with β-D-mannopyranosyl units linked 1–4 with single membered α-D-galactopyranosyl units occurring as side branches. GG and their derivatives have been used in many areas (e.g. thickening agent, ion exchange resin and suspending agent etc.). However, little information regarding the application of GG in superabsorbent fields was reported.

Recently, natural inorganic clays have been widely utilized in superabsorbent fields for improving performance and reducing cost. However, they are poorly suited to mixing and interacting with most polymer matrices. For this reason, clay must be treated before it was used to make a better dispersion. A popular and relatively easy method making clays more compatible with organic matrix is surface modifying, ion exchanging and organification (Kawasumi, Hasegawa, Kato, Usuki, & Okada, 1997; Pavlidou & Papaspyrides, 2008), and the modified clays also exhibited improved properties than raw ones. Currently, clays commonly used for preparation of polymer matrix nanocomposites are mainly focused on montmorillonite and hectorite (Wang, Zhang, Wu, Yang, & Zhang, 2005). Rectorite (REC) is a particular clay mineral. It is a sort of regularly interstratified clay mineral with alternate pairs

* Corresponding author. Tel.: +86 931 4968118; fax: +86 931 8277088.
E-mail address: aqwang@lzb.ac.cn (A. Wang).

0144-8617/$ - see front matter © 2009 Elsevier Ltd. All rights reserved.
doi:10.1016/j.carbpol.2009.03.012

of a non-expansible dioctahedral mica-like layer and an expansible dioctahedral smectitelike layer existing in a 1:1 ratio (Wang et al., 2006). The interlayer cations of montmorillonite-like layers can be exchanged easily by either organic or inorganic cations, and therefore rectorite has the similar water-swelling property to montmorillonite. So it is possible to form monolithic REC layers with the thickness of a single rectorite platelet is about 2 nm and to prepare nanocomposites by exfoliation and intercalation techniques (Ma, Liang, Liu, Fei, & Huang, 2005; Yu, Cui, Wei, & Huang, 2007). It is expected that the superabsorbent nanocomposites with improved performance could be obtained through introducing GG and modified REC synchronously.

On the basis of above description, in this work, the series of guar gum-*g*-poly(sodium acrylate)/rectorite (GG-*g*-PNaA/REC) superabsorbent nanocomposites were prepared by using GG, acidified or organified REC as raw materials. The structure and morphology of nanocomposites were characterized by Fourier transform infrared spectroscopy (FTIR), X-ray diffraction (XRD) and scanning electron microscopy (SEM) techniques. Meanwhile, the effects of HCl concentration, organification degree of CTA^+-REC and content of REC on swelling properties of the developed nanocomposites were also investigated systematically.

2. Experimental

2.1. Materials

Guar gum (GG, food grade, number average molecular weight 220,000) was from Wuhan Tianyuan Biology Co., China. Acrylic acid (AA, chemically pure, Shanghai Shanpu Chemical Factory, Shanghai, China) was distilled under reduced pressure before use. Ammonium persulfate (APS, analytical grade, Xi'an Chemical Reagent Factory, China) was used as received. *N*,*N*′-methylenebisacrylamide (MBA, chemically pure, Shanghai Chemical Reagent Corp., China) was used as purchased. Cetyltrimethylammonium bromide (CTAB) was supplied by Beijing Chemical Reagents Company (Beijing, China). Rectorite (REC) micropowder (Mingliu Colloidal Co., Hubei, China) was milled and passed through a 320-mesh screen prior to use. All other reagents used were of analytical grade and all solutions were prepared with distilled water.

2.2. Preparation of acidified REC

A set of acidified REC (H^+-REC) samples were prepared according to the following procedures: 10.0 g of natural REC powder was dispersed in 100 mL HCl aqueous solution with various concentrations (2, 4, 6, 8 and 12 mol/L), and then the suspension was vigorously stirred (1250 r/min) at room temperature for 4 h. The resultant H^+-REC product was isolated from the suspension by centrifugation and washed with distilled water for several times to remove residual acid and other impurities present until the pH of the washed solution reached 6. The final product was dried to constant weight in an oven at 100 °C and passed through a 320-mesh sieve (46 μm) prior to use.

2.3. Preparation of organified REC

The series of organified REC (CTA^+-REC) samples with various organification degrees were prepared as follows: five different amount of CTAB were dissolved in 100 mL distilled water, respectively. Then, 10.0 g REC was charged into the solution of CTAB and the resultant suspension was vigorously stirred at room temperature for 4 h. The generated CTA^+-REC product was separated by suction filtration and washed with huge volumes of distilled water to remove superfluous CTAB until no Br^- can be detected by 0.1 mol/L $AgNO_3$ solution from the filtrate. Finally, the CTA^+-REC was dried to constant weight in an oven at 100 °C for 6 h and passed through a 320-mesh sieve (diameter is about 46 μm).

The organification degree of CTA^+-REC (denotes the weight percent of organic cation in CTA^+-REC sample) was determined by thermogravimetric analysis: the dried CTA^+-REC sample (0.50 g) modified by different amount of CTAB and raw REC sample (0.50 g) was placed in the crucible after being accurately weighed, respectively. Then, the crucible was calcined in air at 800 °C for 6 h. After reaching a constant weight, the samples were transferred into a desiccator and cooled to room temperature. Finally, these samples were weighed and the organification degree of CTA^+-REC was calculated according to Eqs (1) and (2).

$$\mathrm{OD} = (h - p)/m_1 \times 100\% \quad (1)$$

$$h \text{ or } p = m_1 - m_2 \quad (2)$$

where OD is the organification degree of CTA^+-REC; h and p are the weight loss of CTA^+-REC and raw REC, respectively; m_1 and m_2 are the weight of the samples before and after calcining, respectively. The dosage of CTAB and corresponding organification degree of CTA^+-REC was corresponded as follows (Dosage of CTAB/Organification degree): 0.4992 g/2.49 wt%; 0.9984 g/6.34 wt%; 1.9968 g/9.67 wt%; 2.4959 g/12.34 wt%; 2.9952 g/15.13 wt%.

2.4. Preparation of GG-g-PNaA/REC and GG-g-PNaA superabsorbents

GG (1.20 g) was dispersed in 34 mL of NaOH solution (pH 12.5, 0.067 mol/L) in a 250-mL four-necked flask equipped with a mechanical stirrer, a reflux condenser, a thermometer and a nitrogen line. The resulting dispersive mixture was heated to 60 °C in an oil bath for 1 h to form colloidal slurry. Then, the aqueous solution (4 mL) containing initiator APS (0.1008 g) was added to the slurry and continuously stirred at 60 °C for 10 min to generate radicals. A 7.2 g of acrylic acid was neutralized using 8.5 mL 8 mol/L NaOH to reach a total neutralization degree of 70% (34 mL 0.067 mol/L NaOH solution used to disperse GG was calculated as a part of neutralization degree), and then 28.8 mg crosslinker MBA and 0.95 g of REC micropowder was charged into the neutralized acrylic acid under magnetic stirring, forming a uniform mixture solution. After the reactants were cooled to 40 °C, the mixture solution was added into the reaction flask, and then the oil bath was slowly heated to 70 °C and kept for 3 h to finish polymerization. A nitrogen atmosphere was maintained throughout the reaction period. The obtained gel products were dried to constant weight in an oven at 70 °C; the dried samples were ground and passed through 40–80 mesh sieve (180 ~ 380 μm). GG-*g*-PNaA superabsorbent hydrogel was prepared according to a similar procedure except without REC.

2.5. Measurements of equilibrium water absorbency and swelling kinetics

A 0.05 g of dry sample was immersed in excessive aqueous liquid at room temperature for 4 h to reach swelling equilibrium. The swollen gels were filtered using a mesh screen, and then drain on the sieve for 10 min until no redundant water can be removed. After weighing the swollen samples, the equilibrium water absorbency of the superabsorbent was calculated using Eq. (3).

$$Q_{eq} = (w_2 - w_1)/w_1 \quad (3)$$

Q_{eq} is the equilibrium water absorbency calculated as grams of water per gram of the sample, which are the averages of three measurements; w_1 and w_2 are the weights of the dry sample and water-swollen sample, respectively.

Swelling kinetics of superabsorbents in distilled water was measured as follows: an accurate amount of samples (0.05 g) were

placed in 500 mL beakers, and then 200 mL of distilled water was poured into the beakers. The swollen gels were filtered using a sieve at set intervals (1, 3, 5, 8, 10, 15, 20, 30 and 60 min), and the water absorbency of superabsorbents at a certain moment was measured by weighing the swollen and dry samples and was calculated according to Eq. (3). All samples were carried out three times repeatedly and the averages are reported in this paper.

2.6. Characterizations

FTIR spectra were recorded on a Nicolet NEXUS FTIR spectrometer in 4000–400 cm^{-1} region using KBr pellets. XRD analyses were performed using an X-ray power diffractometer with Cu anode (PAN analytical Co. X'pert PRO), running at 40 kV and 30 mA, scanning from 1.6° to 15°. The morphologies of the samples were examined using a JSM-5600LV SEM instrument (JEOL) after coating the sample with gold film. The BET specific surface area and average pore size of the samples were measured using an Accelerated Surface Area and Porosimetry System (Micromeritics, ASAP 2020) by BET-method at 76 K.

3. Results and discussion

3.1. FTIR spectra

The FTIR spectra of raw REC, modified REC and superabsorbent nanocomposites were shown in Fig. 1. As can be seen from Fig. 1(a and b), the new peak at 3678 cm^{-1} (stretching vibration of —OH groups on REC surface) appeared in the spectrum of H^+-REC after acidification. The Si—O stretching vibration peak at 1121 cm^{-1} was strengthen after acidification, indicating that the amounts of Si—OH were increased after acidification. It can be noticed from Fig. 1(c) that a batch of new peaks at 2917, 2848 and 1471 cm^{-1} (the asymmetrical stretching vibration, symmetrical stretching vibration and bending vibration of $—CH_3$ and $—CH_2$ groups) appeared in the spectrum of CTA^+-REC. This result indicates that organic cations of CTAB have exchanged with the interlayer Ca^{2+} of REC and REC was organified by surfactant CTAB (Wang et al., 2006).

It can be seen from Fig. 1(d), the absorption bands of GG at 1017, 1082 and 1158 cm^{-1} are ascribed to the stretching vibrations

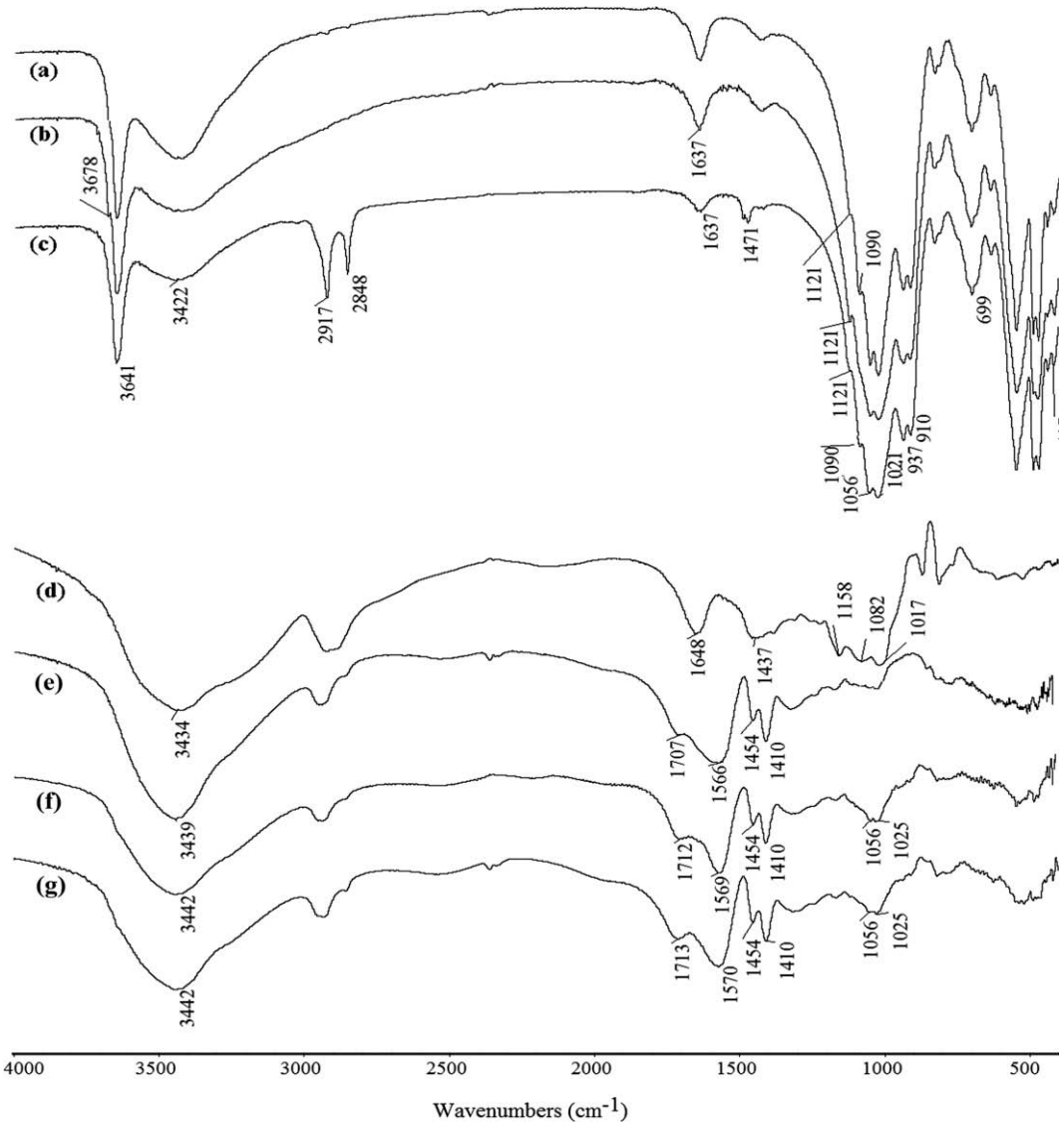

Fig. 1. The FTIR spectra of (a) raw REC, (b) H^+-REC (C_{HCl} = 2 mol/L), (c) CTA^+-REC (OD = 9.67 wt%), (d) GG, (e) GG-*g*-PNaA, (f) GG-*g*-PNaA/H^+-REC (C_{HCl} = 2 mol/L; Content, 10 wt%) and (g) GG-*g*-PNaA/CTA^+-REC (OD = 9.67 wt%; Content, 10 wt%).

of C—O(H) and the band at 1648 cm^{-1} is ascribed to bending vibration of —OH groups. However, these absorption peaks of GG almost disappeared and the new peaks at about 1566, 1454 and 1410 cm^{-1} (asymmetric stretching and symmetric stretching in $—COO^-$ groups, respectively) appeared in the spectra of GG-*g*-PNaA, GG-*g*-PNaA/H^+-REC and GG-*g*-PNaA/CTA^+-REC after grafting copolymerization with NaA (Fig. 1(e–g)). This observation reveals that NaA had been grated onto GG backbone. In addition, the —OH stretching vibration at 3678, 3641 and 3422 cm^{-1} for H^+-REC, at 3641 and 3422 cm^{-1} for CTA^+-REC and the —OH bending vibration of REC at 1637 cm^{-1} almost disappeared after reaction (Fig. 1(f and g)). The absorption bands of REC at 1056 and 1021 cm^{-1} attributed to ≡Si—O stretching appeared in the spectra of GG-*g*-PNaA/REC and are obviously weakened after reaction. These informations indicate that the REC also participated in the grafting copolymerization reaction through its active ≡Si—OH groups (Li, Wang, & Chen, 2004).

3.2. XRD analyses

XRD patterns of raw REC, H^+-REC, CTA^+-REC, GG-*g*-PNaA/H^+-REC (10 and 20 wt%) and GG-*g*-PNaA/CTA^+-REC (10 wt%) were collected from 1.6° to 15° (2θ) and are shown in Fig. 2(a–h). It can be observed that raw REC shows a strong (001) diffraction peak at 2θ = 3.61° with a basal spacing (*d*) of 2.46 nm and a (002) diffraction peak at 2θ = 7.24° (*d* = 1.22 nm). After being treated using HCl solution with lower concentration, the (001) and (002) characteristic peak has no obvious change compared with raw REC (Fig. 2(b and c)), indicating that the crystal structure of REC has not been destroyed during acidification. However, when the concentration of HCl solution reaching 12 mol/L, the (001) and (002) characteristic peak of REC shifted to 2θ = 3.65° (*d* = 2.42 nm) and 2θ = 7.28° (*d* = 1.21 nm), respectively.

It can be observed from Fig. 2, the (001) and (002) diffraction peaks shifted to 2θ = 2.95° (*d* = 3.00 nm) and 2θ = 5.96° (*d* = 1.48 nm) after being organified using CTAB, indicating that CTA^+ have been intercalated into the gallery of REC and the layer gap was expanded. After polymerizing with GG and NaA, the (001) and (002) diffraction peaks disappeared in the XRD curves of GG-*g*-PNaA/H^+-REC even the content of H^+-REC reaching 20 wt% (Fig. 2(g and h)). And the (001) characteristic peak shifted to 2θ = 2.26° (*d* = 3.91 nm) in the XRD curves of GG-*g*-PNaA/CTA^+-REC. As known, the changes in data of crystallochemical parameters derived from (001) peak analysis is the criterion, by which the intercalated or exfoliated composite can be decided (Burnside & Giannelis, 1995). Therefore, the absence of (001) diffraction peaks of GG-*g*-PNaA/H^+-REC and the shift of (001) peaks of GG-*g*-PNaA/CTA^+-REC to lower angle after reaction show that H^+-REC was exfoliated (Scheme 1(a)) and CTA^+-REC was intercalated by polymer chains (Scheme 1(b)), the REC layers are uniformly dispersed in the polymer matrix at nano size (Al, Güçlü, İyim, Emik, & Özgümüş, 2008; Liu et al., 2007a).

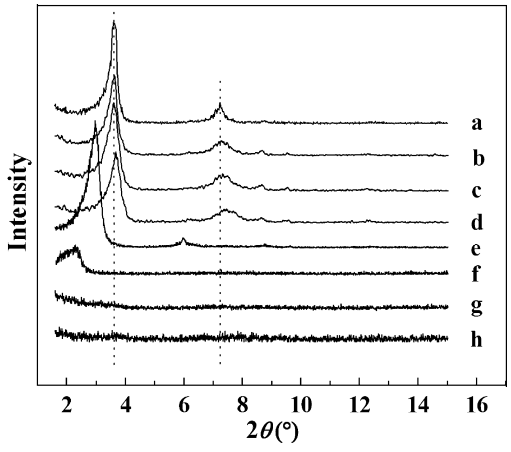

Fig. 2. XRD patterns of (a) raw REC, (b) H^+-REC (C_{HCl} = 2 mol/L), (c) H^+-REC (C_{HCl} = 6 mol/L), (d) H^+-REC (C_{HCl} = 12 mol/L), (e) CTA^+-REC (OD = 9.67 wt%), (f) GG-*g*-PNaA/CTA^+-REC (OD = 9.67 wt%; Content, 10 wt%), (g) GG-*g*-PNaA/H^+-REC (C_{HCl} = 2 mol/L; Content, 10 wt%) and (h) GG-*g*-PNaA/H^+-REC (C_{HCl} = 2 mol/L, Content; 20 wt%).

3.3. Morphological SEM

SEM micrographs of GG-*g*-PNaA, GG-g-PNaA/H^+-REC, and GG-*g*-PNaA/CTA^+-REC superabsorbent nanocomposites containing 10 wt% of H^+-REC or CTA^+-REC were observed and are shown in Fig. 3. As can be seen from Fig. 3(a), the GG-*g*-PNaA superabsorbent hydrogel only exhibits a smooth and dense surface; while the nanocomposites containing H^+-REC or CTA^+-REC all show a relatively coarse and undulant surface (Fig. 3(b, c)). Also, some pores can be observed in the surface of GG-*g*-PNaA/CTA^+-REC and the surface roughness GG-*g*-PNaA/CTA^+-REC superabsorbents is obviously higher than that of GG-*g*-PNaA/H^+-REC, which implies that

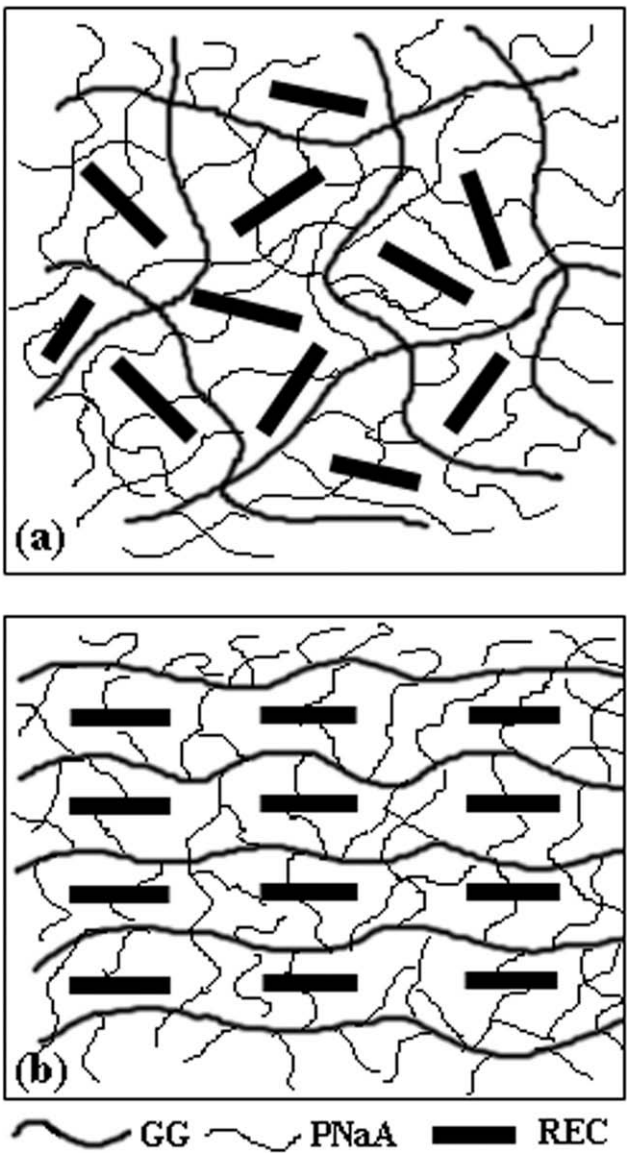

Scheme 1. Schematic illustration of (a) exfoliated nanocomposite GG-g-PNaA/H^+-REC and (b) intercalated nanocomposite GG-*g*-PNaA/CTA^+-REC.

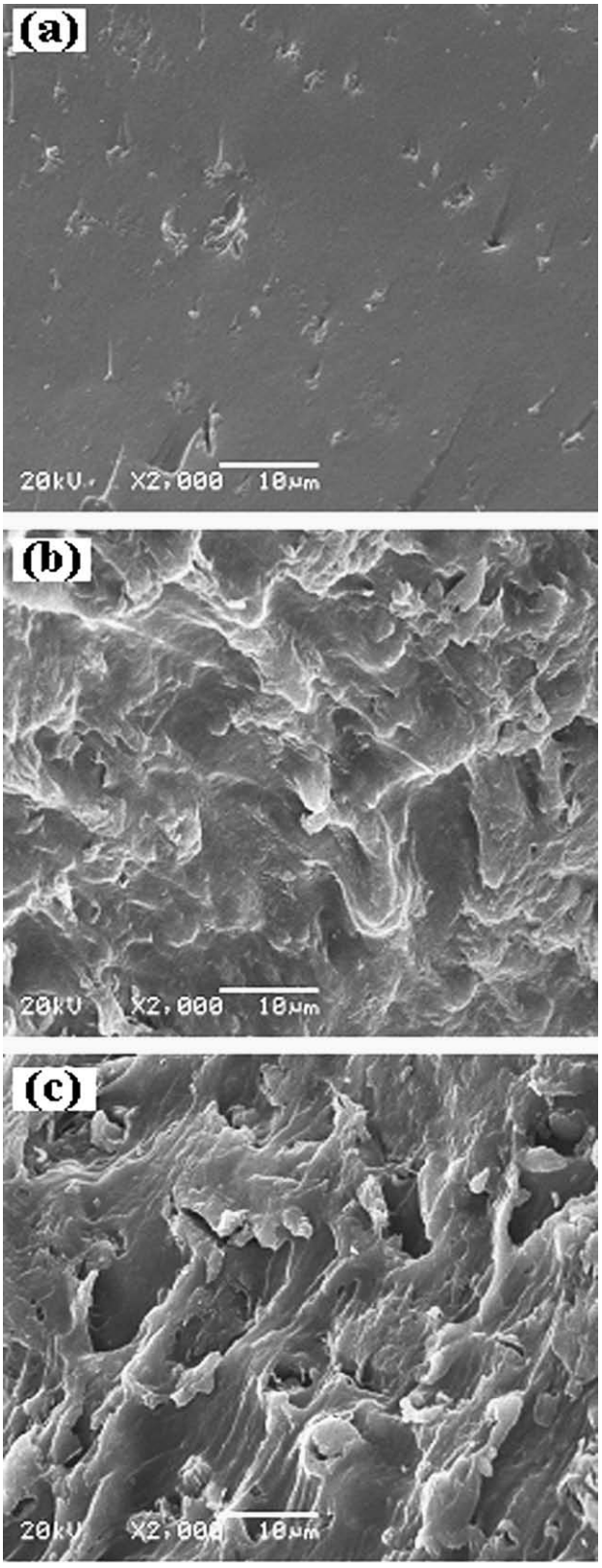

Fig. 3. SEM micrographs of (a) GG-*g*-PNaA, (b) GG-*g*-PNaA/H^+-REC (C_{HCl} = 2 mol/L; Content, 10 wt%) and (c) GG-*g*-PNaA/CTA^+-REC (OD = 9.67 wt%; Content, 10 wt%).

modifying REC by CTAB is more favorable to improve the surface structure of nanocomposite. Moreover, the degree of dispersion of clay micropowder in the polymer matrix is more important for an organic–inorganic composite (Santiago, Mucientes, Osorio, & Rivera, 2007). As shown in Fig. 3, the REC are dispersed in the polymer matrix more uniformly and almost embedded within GG-*g*-PNaA in superabsorbent nanocomposites (Fig. 3(b and c)), and no flocculation of REC particles was observed. The fine dispersion of H^+-REC and CTA^+-REC particles in polymeric network by exfoliated and intercalated mode facilitates the superabsorbent to form a homogeneous composition, and the observation result is accordant with the XRD results (Fig. 2).

3.4. Effects of HCl concentration on water absorbency

The concentration of HCl solution used for modifying REC has great influence on the water absorbency of the resultant nanocomposites. As shown in Fig. 4, the water absorbency of GG-*g*-PNaA/H^+-REC decreased with increasing the concentration of HCl solution from 2 to 6 mol/L, and then increased with further increase in HCl concentration. In order to evaluate the change of physical parameter of REC before and after acidification, the BET specific surface area and average pore size were determined and shown in Table 1. It can be noticed that the BET specific surface area and average pore size of H^+-REC are all higher than that of raw REC. This indicates that treating REC using HCl solution may decompose the mineral congeries and dredge the channel and increase the specific surface area of REC. In addition, the removal of impurity among REC particles makes the covered Si—OH exposed out. As a result, the amounts of active Si—OH groups on REC surface increased (see FTIR results) and the affinity of REC with polymeric matrix was enhanced. Because active Si—OH groups may participate in constructing polymeric network, the collaborative action of specific surface area and active Si—OH groups contributes to improve the water absorbency in a suitable HCl concentration (2 mol/L). As HCl concentration increase, more H^+ can exchange the cations on the surface of REC. As a result, the amount of active cation site reduced and polymeric networks fail to be formed well (Wang, Zhang, Chen, & Wang, 2007), and thus

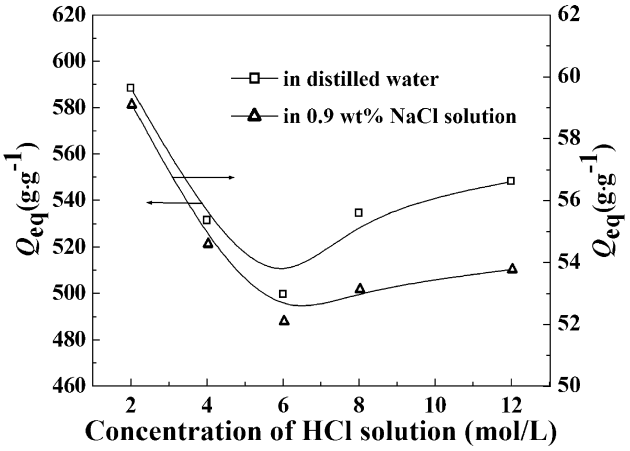

Fig. 4. Variation of equilibrium water absorbency for the GG-*g*-PNaA/H^+-REC (10 wt%) superabsorbent nanocomposite with HCl concentration.

Table 1
The BET specific surface area and the average pore size for REC acidified by HCl solution with various concentrations.

HCl concentration (mol/L)	BET specific surface area ($m^2\ g^{-1}$)	Average pore width (4 V/A by BET) (nm)
0	12.5352	7.6282
2	15.0303	9.8206
4	16.7230	9.9885
6	15.1234	10.9189
8	17.2880	10.2329
12	17.3238	10.8512

the water absorbency decreased. When the concentration of HCl solution exceeding 6 mol/L, H^+ ion can exchange with the divalent basic metal ion, which increased the water-swelling properties of REC (Zanetti, Lomakin, & Camino, 2000) and contribute to improve the water absorbency.

3.5. Effects of organification degree of CTA^+-REC on water absorbency

Like HCl concentration, the organification degree of CTA^+-REC has also greater influence on the water absorbency of nanocomposite. As shown in Fig. 5, the water absorbency of superabsorbent nanocomposite containing 10 wt% CTA^+-REC at each organification degrees is always higher than that of GG-*g*-PNaA/raw-REC. The water absorbency increased with the increase of organification degree, reaching a maximum absorption (608 g g^{-1}) at the optimum organification degree of 9.67 wt% and then decreased. After REC being organified, the long alkyl chains of CTA^+ ion can intercalate into the gallery of REC layers or attach on the surface of REC, which can form tiny hydrophobic regions. Thus, the hydrogen bond interaction between hydrophilic polymeric chains containing —COOH and $—COO^-$ groups was weaken and intertwist of polymer chains was also prevented. As a result, the polymeric network can be regularly formed. In addition, the intercalation of CTA^+ expands the layer gap and lowered the negative charges in the REC surface. The polymeric chains can be intercalated into REC gallery and form a nanocomposite structure. Thus, the REC can be uniformly dispersed in the polymer, and the better dispersion of REC contributes to improve polymeric network and then enhance water absorbency. In addition, the long alkyl chains can act as obstructers for the radical polymerization reaction, the opportunity for cyclization reaction of MBA increases and then the network is also less crosslinked and therefore swells more (Elliott, Macdonald, Nie, & Bowman, 2004).

However, when the organification degree of CTA^+-REC exceeding 9.67 wt%, the amount of hydropholic alkyl chains increased in polymeric network; on one hand, this restricted activity of surface —OH of REC and then affected the grafting efficiency of REC; on the other hand, the increase of alkyl chains also lowered the hydrophilicity of the polymer, and then lead to the shrinkage of water absorbency of the corresponding superabsorbent nanocomposite. Therefore, the maximum water absorbency can only be obtained when REC clay was modified with a suitable organification degree.

3.6. Effects of H^+-REC and CTA^+-REC content on water absorbency

Content of REC may decide the composition and structure of the nanocomposites, and thus affected their water absorbency. As shown in Fig. 6, the water absorbencies of the nanocomposites increased with increasing the content of H^+-REC and CTA^+-REC, reaching a maximum at 10 wt% and then decreased. It is well known that REC contains large amounts of active —OH groups on its platelet surface. Since the H^+-REC clay was exfoliated and CTA^+-REC was intercalated during polymerization, the well-dispersed REC platelets can effectively participate in grafting copolymerization reaction through active surface —OH groups. As a result, the incorporation of rigid REC platelets into polymeric network prevent intertwist of graft polymeric chains and weaken the hydrogen-bonding interaction among —COOH groups, and then decreased the physical crosslinking degree and improved polymeric network. Thus, the water absorbency can be enhanced with introducing moderate amount of modified REC. However, the dispersed REC can act as an additional crosslinking point in the polymeric network (Lin, Wu, Yang, & Pu, 2001) when the content of modified REC exceeding 10 wt%. Thus, the introduction of REC into polymeric network may increase the crosslinking density of composite and minimize the network space for holding water. Moreover, the platelets of REC may physically stack in the network space when introducing excess REC, which decreased the ratio of hydrophilic groups in unit volume and lead to the decrease of hydrophilicity of nanocomposite. Thus, the water absorbency decreased with the further increase of REC content.

3.7. Swelling kinetics

The incorporation of different REC certainly affects the swelling kinetics of the resulting superabsorbents. The kinetic determination results show that the swelling rate of the superabsorbents with certain particle sizes ($180 \sim 380\ \mu m$) is higher within 10 min. Later, the swelling rate is reduced, and the curves of the swelling rate become flatter. In this section, the swelling kinetics can be expressed by the Voigt-based viscoelastic model (Eq. (4)) (Kabiri, Omidian, Hashemi, & Zohuriaan-Mehr, 2003; Omidian, Hashemi, Sammes, & Meldrum, 1998).

$$Q_t = Q_\infty(1 - e^{-t/r}) \tag{4}$$

where Q_t (g g^{-1}) is swelling capability at time t, Q_∞ (g g^{-1}) is the power parameter (g g^{-1}), denoting the theoretical equilibrium water absorbency; t(min) is time for swelling Q_t, and r (min) stand for the "rate parameter", denoting the time required to reach 0.63 of equilibrium water absorbency. The data obtained from the equilibrium water absorbency and the swelling rate for each sample was fitted into the Eq. (4) to obtain the rate parameter r and power parameter Q_∞. It was calculated that the r values are 4.38, 4.36

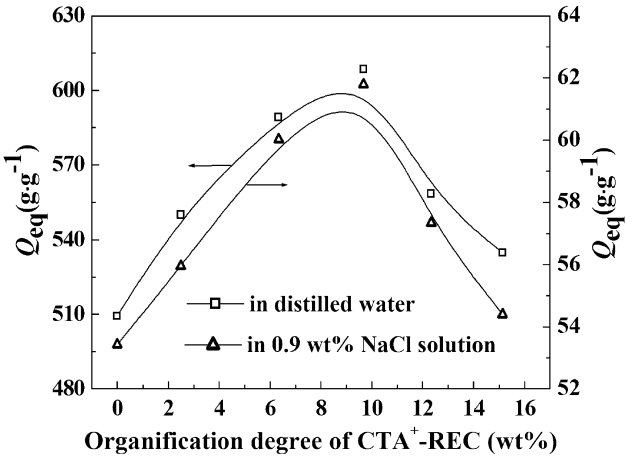

Fig. 5. Variation of equilibrium water absorbency for GG-*g*-PNaA/CTA^+-REC (10 wt%) superabsorbent nanocomposite with organification degree of CTA^+-REC.

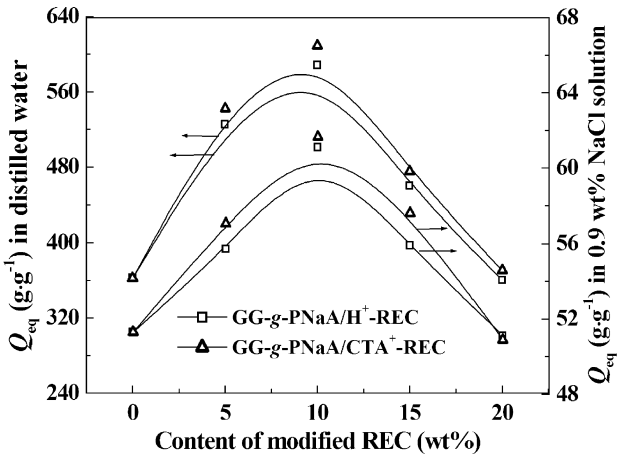

Fig. 6. Effect of H^+-REC (C_{HCl} = 2 mol/L) and CTA^+-REC (OD = 9.67 wt%) content on the water absorbency.

and 3.39 min; the p values are 357, 591 and 601 g g^{-1} for GG-g-PNaA, GG-g-PNaA/H^+-REC (C_{HCl} = 2 mol/L; Content, 10 wt%) and GG-g-PNaA/CTA^+-REC (OD = 9.67 wt%; Content, 10 wt%), respectively. Because the rate parameter r is a measure of resistance to water permeation, a lower r value will reflect a higher swelling rate (Pourjavadi & Mahdavinia, 2006), it is obvious that the swelling rate for each sample is as following orders: GG-g-PNaA/CTA^+-REC (OD = 9.67 wt%; Content, 10 wt%) > GG-g-PNaA/H^+-REC (C_{HCl} = 2 mol/L; Content, 10 wt%) > GG-g-PNaA. This result indicates that the organification treatment of raw REC is favorable to improve the swelling rate of the resultant superabsorbent nanocomposites.

4. Conclusions

The series of exfoliated and intercalated superabsorbent nanocomposites based on natural guar gum, acidified and organified REC were prepared through solution polymerization. FTIR, XRD and SEM analysis indicates that REC was exfoliated for H^+-REC and was intercalated for CTA^+-REC during polymerization, and REC platelets were uniformly dispersed in GG-g-PNaA matrix. The dispersed platelets participate in the polymerization reaction through active —OH groups on their surface. Modifying REC by acidification and organification can greatly improve the water absorbencies of corresponding superabsorbent nanocomposites. Organified REC can improve the swelling capabilities and swelling rate to a greater degree contrast to acidified REC. The superabsorbent nanocomposites based on renewable and biodegradable natural GG and modified inorganic REC clay resources exhibited improved swelling capability and swelling rate, which can be used as promising water-manageable materials for various application.

Acknowledgements

This work was financially supported by the Western Action Project of CAS (No. KGCX2-YW-501) and "863" Project of the Ministry of Science and Technology, PR China (No. 2006AA03Z0454 and 2006AA100215).

References

Al, E., Güçlü, G., İyim, T. B., Emik, S., & Özgümüş, S. (2008). Synthesis and properties of starch-*graft*-acrylic acid/Na-montmorillonite superabsorbent nanocomposite hydrogels. *Journal of Applied Polymer Science, 109*, 16–22.

Burnside, S. D., & Giannelis, E. P. (1995). Synthesis and properties of new poly (dimethylsiloxane) nanocomposites. *Chemistry of Materials, 7*, 1597–1600.

Chen, Y., Liu, Y. F., Tan, H. M., & Jiang, J. X. (2009). Synthesis and characterization of a novel superabsorbent polymer of N, O-carboxymethyl chitosan graft copolymerized with vinyl monomers. *Carbohydrate Polymers, 75*, 287–292.

Chu, M., Zhu, S. Q., Li, H. M., Huang, Z. B., & Li, S. Q. (2006). Synthesis of poly(acrylic acid)/sodium humate superabsorbent composite for agricultural use. *Journal of Applied Polymer Science, 102*, 5137–5143.

Elliott, J. E., Macdonald, M., Nie, J., & Bowman, C. N. (2004). Structure and swelling of poly(acrylic acid) hydrogels: Effect of pH, ionic strength, and dilution on the crosslinked polymer structure. *Polymer, 45*, 1503–1510.

Hua, S. B., & Wang, A. Q. (2009). Synthesis, characterization and swelling behaviors of sodium alginate-*g*-poly(acrylic acid)/sodium humate superabsorbent. *Carbohydrate Polymers, 75*, 79–84.

Kabiri, K., Omidian, H., Hashemi, S. A., & Zohuriaan-Mehr, M. J. (2003). Synthesis of fast-swelling superabsorbent hydrogels: Effect of crosslinker type and concentration on porosity and absorption rate. *European Polymer Journal, 39*, 1341–1348.

Kamat, M., & Malkani, R. (2003). Disposable diapers: A hygienic alternative. *Indian Journal of Pediatrics, 70*, 879–881.

Kaşgöz, H., Durmus, A. Z., & Kaşgöz, A. (2008). Enhanced swelling and adsorption properties of AAm-AMPSNa/clay hydrogel nanocomposites for heavy metal ion removal. *Polymers for Advanced Technologies, 19*, 213–220.

Kawasumi, M., Hasegawa, N., Kato, M., Usuki, A., & Okada, A. (1997). Preparation and mechanical properties of polypropylene–clay hybrids. *Macromolecules, 30*, 6333–6338.

Kosemund, K., Schlatter, H., Ochsenhirt, J. L., Krause, E. L., Marsman, D. S., & Erasala, G. N. (2009). Safety evaluation of superabsorbent baby diapers. *Regulatory Toxicology and Pharmacology, 53*, 81–89.

Lanthong, P., Nuisin, R., & Kiatkamjornwong, S. (2006). Graft copolymerization, characterization, and degradation of cassava starch-*g*-acrylamide/itaconic acid superabsorbents. *Carbohydrate Polymers, 66*, 229–245.

Li, A., Wang, A. Q., & Chen, J. M. (2004). Studies on poly(acrylic acid)/attapulgite superabsorbent compositeI. Synthesis and characterization. *Journal of Applied Polymer Science, 92*, 1596–1603.

Li, A., Zhang, J. P., & Wang, A. Q. (2007). Utilization of starch and clay for the preparation of superabsorbent composite. *Bioresource Technology, 98*, 327–332.

Lin, J. M., Wu, J. H., Yang, Z. F., & Pu, M. L. (2001). Synthesis and properties of poly(acrylic acid)/mica superabsorbent nanocomposite. *Macromolecular Rapid Communications, 22*, 422–424.

Liu, P. S., Li, L., Zhou, N. L., Zhang, J., Wei, S. H., & Shen, J. (2007a). Waste polystyrene foam-*graft*-acrylic acid/montmorillonite superabsorbent nanocomposite. *Journal Applied Polymer Science, 104*, 2341–2349.

Liu, J. H., Wang, Q., & Wang, A. Q. (2007b). Synthesis and characterization of chitosan-*g*-poly(acrylic acid)/sodium humate superabsorbent. *Carbohydrate Polymers, 70*, 166–173.

Ma, X. Y., Liang, G. Z., Liu, H. L., Fei, J. Y., & Huang, Y. (2005). Novel intercalated nanocomposites of polypropylene/organic-rectorite/polyethylene-octene elastomer: Rheology, crystallization kinetics, and thermal properties. *Journal of Applied Polymer Science, 97*, 1915–1921.

Omidian, H., Hashemi, S. A., Sammes, P. G., & Meldrum, I. G. (1998). A model for the swelling of superabsorbent polymers. *Polymer, 39*, 6697–6704.

Pavlidou, S., & Papaspyrides, C. D. (2008). A review on polymer-layered silicate nanocomposites. *Progress in Polymer Science, 33*, 1119–1198.

Pourjavadi, A., Barzegar, S., & Mahdavinia, G. R. (2006). MBA-crosslinked Na-Alg/CMC as a smart full-polysaccharide superabsorbent hydrogels. *Carbohydrate Polymers, 66*, 386–395.

Pourjavadi, A., Ghasemzadeh, H., & Soleyman, R. (2007a). Synthesis, characterization, and swelling behavior of alginate-*g*-poly(sodium acrylate)/kaolin superabsorbent hydrogel composites. *Journal of Applied Polymer Science, 105*, 2631–2639.

Pourjavadi, A., Hosseinzadeh, H., & Sadeghi, M. (2007b). Synthesis, characterization and swelling behavior of gelatin-*g*-poly(sodium acrylate)/kaolin superabsorbent hydrogel composites. *Journal of Composite Materials, 41*, 2057–2069.

Pourjavadi, A., & Mahdavinia, G. R. (2006). Superabsorbency, pH-sensitivity and swelling kinetics of partially hydrolyzed chitosan-*g*-poly (acrylamide) hydrogels. *Turkish Journal of Chemistry, 30*, 595–608.

Puoci, F., Iemma, F., Spizzirri, U. G., Cirillo, G., Curcio, M., & Picci, N. (2008). Polymer in agriculture: A review. *American Journal of Agricultural and Biological Sciences, 3*, 299–314.

Ray, S. S., & Bousmina, M. (2005). Biodegradable polymers and their layered silicate nanocomposites: In greening the 21st century materials world. *Progress in Materials Science, 50*, 962–1079.

Sadeghi, M., & Hosseinzadeh, H. J. (2008). Synthesis of starch-poly(sodium acrylate-*co*-acrylamide) superabsorbent hydrogel with salt and pH-responsiveness properties as a drug delivery system. *Journal of Bioactive and Compatible Polymers, 23*, 381–404.

Santiago, F., Mucientes, A. E., Osorio, M., & Rivera, C. (2007). Preparation of composites and nanocomposites based on bentonite and poly(sodium acrylate). Effect of amount of bentonite on the swelling behaviour. *European Polymer Journal, 43*, 1–9.

Suo, A. L., Qian, J. M., Yao, Y., & Zhang, W. G. (2007). Synthesis and properties of carboxymethyl cellulose-*graft*-poly(acrylic acid-*co*-acrylamide) as a novel cellulose-based superabsorbent. *Journal of Applied Polymer Science, 103*, 1382–1388.

Wang, X. Y., Du, Y. M., Yang, J. H., Wang, X. H., Shi, X. W., & Hu, Y. (2006). Preparation, characterization and antimicrobial activity of chitosan/layered silicate nanocomposites. *Polymer, 47*, 6738–6744.

Wang, W. J., Zhang, J. P., Chen, H., & Wang, A. Q. (2007). Study on superabsorbent compositeVIII. Effects of acid- and heat-activated attapulgite on water absorbency of polyacrylamide/attapulgite. *Journal of Applied Polymer Science, 103*, 2419–2424.

Wang, L., Zhang, J. P., & Wang, A. Q. (2008). Removal of methylene blue from aqueous solution using chitosan-*g*-poly(acrylic acid)/montmorillonite superadsorbent nanocomposite. *Colloid Surface A, 322*, 47–53.

Wang, Y. Q., Zhang, H. F., Wu, Y. P., Yang, J., & Zhang, L. Q. (2005). Preparation and properties of natural rubber/rectorite nanocomposites. *European Polymer Journal, 41*, 2776–2783.

Yoshimura, T., Uchikoshi, I., Yoshiura, Y., & Fujioka, R. (2005). Synthesis and characterization of novel biodegradable superabsorbent hydrogels based on chitin and succinic anhydride. *Carbohydrate Polymers, 61*, 322–326.

Yu, J. H., Cui, G. J., Wei, M., & Huang, J. (2007). Facile exfoliation of rectorite nanoplatelets in soy protein matrix and reinforced bionanocomposites thereof. *Journal of Applied Polymer Science, 104*, 3367–3377.

Zanetti, M., Lomakin, S., & Camino, G. (2000). Polymer layered silicate nanocomposites. *Macromolecular Materials and Engineering, 279*, 1–9.

Zhang, J. P., Wang, Q., & Wang, A. Q. (2007). Synthesis and characterization of chitosan-*g*-poly(acrylic acid)/attapulgite superabsorbent composites. *Carbohydrate Polymers, 68*, 367–374.